

## PLASMA ENGINEERING ASSESSMENTS OF COMPACT IGNITION EXPERIMENTS\*

By acceptance of this article, the publisher or recipient acknowledges the U.S. Government's right to retain a nonexclusive, royalty-free license in and to any copyright covering the article.

W. A. Houlberg  
Oak Ridge National Laboratory  
P.O. Box Y  
Oak Ridge, Tennessee 37831

CONF-851102--107

DE86 008979

## Abstract

Confinement, startup sequences, and fast-alpha particle effects are assessed for a class of compact tokamak ignition experiments having high toroidal magnetic fields (8–12 T) and high toroidal currents (7–10 MA). The uncertainties in confinement scaling are spanned through examples of performance with an optimistic model based on ohmically heated plasmas and a pessimistic model that includes confinement degradation by both auxiliary and alpha heating. The roles of neoclassical resistivity enhancement and sawtooth behavior are also evaluated. Copper toroidal field coils place restrictions on pulse lengths due to resistive heating, so a simultaneous rampup of the toroidal field and plasma current is proposed as a means of compressing the startup phase and lengthening the burn phase. If the ignition window is small, fast-alpha particle physics is restricted to the high-density regime where a short slowing-down time leads to low fast-particle density and pressure contributions. Under more optimistic confinement, a larger ignition margin broadens the range of alpha particle physics that can be addressed. These issues are illustrated through examples of transport simulations for a set of machine parameters called BRAND-X, which typify the designs under study.

## I. Introduction

A compact, high-field tokamak has been proposed as an economical means of examining the physics of ignition. Candidate devices include the IGNITOR-A [1], LITE [2], and PPPL-0424 [3]. Their parameters are summarized in Table I. Although these devices are characterized by lower toroidal fields, larger size, and higher plasma currents than the original IGNITOR design [4], they are considerably smaller than TFTR and JET. Sufficient confinement for ignition is attained through higher toroidal fields and plasma currents rather than through size scaling as in earlier TFCX studies [5].

A comprehensive confinement study has been carried out with a global analysis that encompasses the set of devices of Table I [6]. For a wide range of confinement models, the "figure of merit"

parameter  $a_0 B_0^2 / q_0$  gives a good indication of the relative performance of the devices. Direct comparisons between the global and 1½-D WHIST transport calculations show good agreement over the entire range of confinement models and machine parameters covered in these studies [6]. Efforts to compare 1-D and 1½-D models with selected experimental data are in progress [7]. The results presented here are constrained to a single set of machine parameters called "BRAND-X," which is intermediate in size and field strength between the designs under study but has a high plasma current and higher elongation, which could allow for an expanded plasma boundary or divertor region. The performance of such a machine is somewhat better than the "figure of merit" parameter indicates because of the higher elongation [6].

In Sect. II, the steady-state operating contours for two confinement models are used to examine the extent (in density and temperature) of the ignition regime, the role of density and beta limits, and the effects of neoclassical resistivity enhancement and sawtooth behavior. A more extensive analysis of steady-state contours is presented in Ref. 6.

The steady-state contours can be used as a guide for systems studies, but the dynamics of startup, thermal excursions, sawtooth activity, and thermalization of the fast alphas need both time and spatial resolution, that is, 1-D (effective minor radius) or 1½-D (effective minor radius evaluated from 2-D MHD equilibrium solution) time-dependent transport models. The WHIST transport code [8] has been used to examine some of these effects, and the results are presented in Sect. III.

## II. Steady-State Operating Contours

Two confinement models are used to illustrate the potential range of performance of a compact tokamak ignition device. The first of these we designate OH for ohmic scaling (one of several variations of "neo-Alcator" scaling) [9]:

$$\tau_E^{OH} = 0.07 \langle n_{e20} \rangle a_0 R_0^2 q_0 \quad (s),$$

where mks-keV units are used, the subscript 20 designates normalization to  $10^{20} \text{ m}^{-3}$ , and angle brackets designate a volume average. The cylindrical safety factor ( $q_0$ ) has been added to the scaling. This model does not yield the saturation of confinement observed at high density or the degradation of confinement with auxiliary heating and is therefore considered an optimistic model. These effects

\*Research sponsored by the Office of Fusion Energy, U.S. Department of Energy, under Contract No. DE-AC05-84OR21400 with Martin Marietta Energy Systems, Inc.

Table I. Machine and Plasma Parameters for Compact Ignition Studies

	IGNITOR-A	LITE	PPPL-0424	BRAND-X
Major radius $R_0$ (m)	1.0125	1.76	1.621	1.40
Minor radius $a_0$ (m)	0.3875	0.55	0.531	0.50
Elongation $\kappa$	1.67	1.60	1.60	1.80
Triangularity $\delta$	0.3	0.3	0.4	0.2
Toroidal field $B_0$ (T)	12.6	8.5	8.95	10.0
Toroidal current $I$ (MA)	10.0	6.95	7.83	10.0
Safety factor at edge $q_\psi(a_0)$	2.6	2.6	2.6	2.6
Cylindrical safety factor $q_0$	2.0	2.1	2.2	2.0
Maximum density $n_{\max}$ ( $\times 10^{20} \text{ m}^{-3}$ )	9.3	3.4	3.8	5.4
Critical beta $\beta_{\text{crit}}$ (%)	6.0	4.5	5.0	6.0
Figure of merit $a_0 B_0^2 / q_0$ ( $\text{T} \cdot \text{m}^2$ )	31	19	20	25

MASTER

EBS

are incorporated in the Kaye-Goldston empirical model for L-mode global energy confinement [9]:

$$(\tau_E^{KG})^{-2} = (\tau_E^{OH})^{-2} + (\tau_E^{aux})^{-2},$$

$$\tau_E^{aux} = 0.056 \left( \frac{I^{1.24} R_0^{1.65} \kappa^{0.28} (n_{e20})^{0.26} A_i^{0.5}}{P^{0.58} a_0^{0.49} B_0^{0.09}} \right) (s),$$

where the current  $I$  is in megamperes and the total power  $P$  is in megawatts. The isotopic effect  $A_i$  has been added to the original scaling to reflect improved confinement of deuterium plasmas over hydrogen plasmas. The total power includes alpha heating as well as ohmic and auxiliary heating contributions in the following examples, so this represents a fairly pessimistic model.

A conversion of the global confinement results to local electron and ion thermal conductivities is required. There are many possible ways to make this conversion, but analysis of experimental results shows that the thermal conductivity must increase radially to approximately reproduce the observed temperature profiles. In the following analyses the coefficients for anomalous thermal conductivity are expressed in terms of global parameters, while the radial form factor

$$g(\hat{\rho}) = \frac{1 + 4\hat{\rho}^2}{2}, \quad 0 \leq \hat{\rho} = \rho/a_0 \leq 1,$$

is used to set the profile shape. An alternative approach is to use the radial variation of local parameters (usually density) to provide the radial increase in the conductivity [7].

The choice of a radial metric  $\rho$  modifies the relationship between transport coefficients and net confinement times. A form for the conduction (and, similarly, convection) terms is given by

$$\frac{3}{2} \frac{\partial nT}{\partial t} = - \frac{1}{V(\rho)} \frac{\partial}{\partial \rho} \left[ V(\rho) \langle (\nabla \rho)^2 \rangle_{\psi} n \chi \frac{\partial T}{\partial \rho} \right] + \dots,$$

where  $V$  is the volume contained within a flux surface and the prime designates the derivative with respect to  $\rho$ .  $\rho$  can formally be any "radial" coordinate—dimensional or dimensionless—so the flux-surface-averaged quantity  $\langle (\nabla \rho)^2 \rangle_{\psi}$  provides a conversion to real space using the assumption that the average gradients over a surface drive the fluxes. If the radial coordinate is taken as  $0 \leq \rho \leq a_0$ , as in the WHIST code, then

$$\langle (\nabla \rho)^2 \rangle_{\psi} = (1 + \kappa^2)/2a^2,$$

which gives a decrease in conduction losses (an improvement in confinement) with increasing elongation for a fixed minor radius in the midplane ( $a_0$ ). Dividing an empirical transport coefficient by this quantity removes the implied scaling with elongation.

Finally, the relative roles of electron and ion confinement must be addressed in the conversion to local, two-fluid thermal conductivities. We use the Chang-Hinton formulation for ion neoclassical conductivity [10] and add a portion of the anomalous losses to the ions instead of using a neoclassical multiplier for the ion neoclassical conductivity:

$$\chi_i = \chi_i^{CH} + 0.2\chi_e^{an}.$$

Similarly, for the particle diffusivity:

$$D = D^{NC} + 0.2\chi_e^{an}.$$

For ohmic scaling, the global results are recovered with

$$\chi_e^{an} = \chi_e^{OH} = 1.2 \left( \frac{a_0^2}{4\tau_E^{OH}} \right) \frac{2\kappa^2}{1 + \kappa^2} g(\rho),$$

while for L-mode scaling

$$\chi_e^{an} = \chi_e^{KG} = 1.9 \left( \frac{a_0^2}{4\tau_E^{KG}} \right) \frac{2\kappa^2}{1 + \kappa^2} g(\rho).$$

Figure 1 shows the steady-state auxiliary power contours for the optimistic OH scaling in the BRAND-X machine. These were generated by the WHIST transport code using the Plasma Operating CONtour (POPCON) option for driving the time-dependent equations to equilibrium [8]. A Gaussian heating profile with a 0.3-m half-width was used to simulate ICRF heating. The division of power between electrons and ions was taken as 25%/75%, although this has no real effect on the results because of the tight coupling between thermal ions and electrons.  $Z_{eff} = 1.5$  was maintained with carbon as the impurity. Neoclassical electrical resistivity enhancement [11] was used to evaluate the ohmic heating and current density evolution. Current density in the core is limited by a discrete sawtooth model, which triggers at  $q(0) < 0.95$  and leads to some fluctuations in the auxiliary power contours. The maximum density is given by the Murakami limit [12]

$$n_{max} = 1.5B_0/R_0q_0 \times 10^{20} \text{ (m}^{-3}\text{)},$$

which may be somewhat high for the ohmic heating phase but should be easier to maintain with auxiliary and internal fusion heating. The best results obtained experimentally under this scaling are better represented by a scaling factor of 2.0 rather than 1.5. Nonetheless, the optimal density for startup lies comfortably below this limit in the region where the ohmic equilibrium and ignition contours are nearest each other.

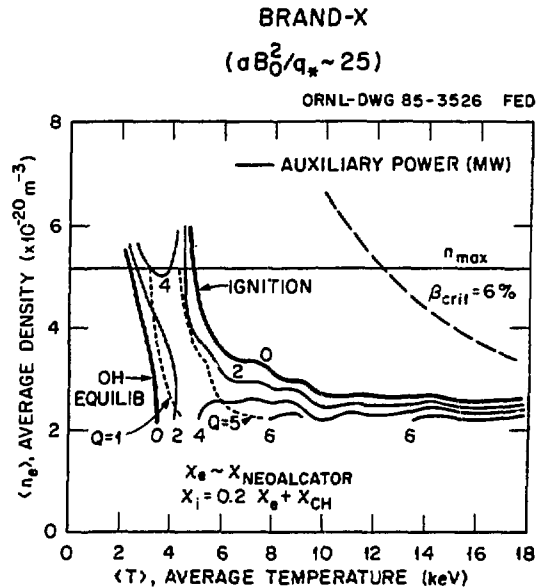


Fig. 1. Steady-state auxiliary power contours for BRAND-X with ohmic scaling. Reference beta and density limits are used to define the large operating regime.

For each of the compact ignition devices of Table I, the saddle point appears at  $(n_e) \approx (0.6-0.8)n_{max}$ . This is where ion conduction plus radiation losses (increasing with density) are comparable to electron conduction losses (decreasing with density). The minimum auxiliary power to reach ignition (applied over an infinitely long time) is about 3 MW. In dynamic simulations the power can be greater than this (finite startup time) or less, depending on the dynamics of the sawtooth activity. Also shown is the Troyon beta limit [13], given by

$$\beta_{crit} \approx 3I/a_0 B_0 \text{ (\%)} ,$$

where the current is in megamperes. The ignition window, bounded by the ignition curve and the density and beta limits, is large.

The neoclassical resistivity enhancement adds 4-5 MW to the ohmic heating in the vicinity of the saddle point and therefore leads to the relatively low auxiliary power requirements for startup. This enhancement has been confirmed in JET discharges, in which the low aspect ratio of the plasma makes the effect more dramatic than in other devices [14]. In compact ignition devices, ohmic heating is a factor of 2-3 higher than would be expected from Spitzer resistivity.

Sawtooth activity, on the other hand, limits the current density in the plasma center and therefore provides a limit on the ohmic heating. Some of this loss is compensated by a conversion of poloidal magnetic energy to plasma kinetic energy during the sawtooth crash and is included in the dynamic simulation of the sawtooth activity. Extrapolation of existing sawtooth models into this regime may produce restrictions on an assessment of ohmic heating to ignition that do not exist. In the vicinity of the saddle point, a relatively small drop in the temperature and density from a sawtooth crash translates to a very large drop in the fusion rate because it occurs where the fusion cross section is rising very rapidly with temperature. If the sawtooth period is long enough or if  $q(0)$  drops low enough, then the plasma may dynamically tunnel through this regime, which appears impassable with a steady-state analysis.

Figure 2 shows the auxiliary power contours for the Kaye-Goldston model. The ignition window still exists but is significantly

reduced because of the reduction of confinement by auxiliary and alpha heating. As mentioned earlier, the density limit may be considerably higher than indicated, so a larger operating margin is likely to exist. This model is probably more realistic than the OH model because it acknowledges experimental evidence of confinement degradation, but its use of L-mode (factor of 2 reduction in confinement from H-mode) and extension of the degraded confinement to alpha heating tend to put the results on the pessimistic side of reality. Designing the device with divertor or expanded boundary capabilities may help push the scaling toward H-mode and yield a larger ignition window.

All of the features of these contours can be generated by a global analysis using appropriate profiles and the fact that the plasma behaves as a single fluid ( $T_e \approx T_i$ ) because of the high density [6]. The dynamics of startup and operation, however, require a more comprehensive time-dependent analysis.

### III. Dynamics of Startup and Operation

Resistive heating of the toroidal field coils may provide the limitation on total pulse length in a compact ignition device with copper coils. A normal startup that takes the toroidal field coils to maximum current, followed by plasma initiation and ramping the plasma current, can easily exceed the total pulse length limitation. To avoid disruptions (presumably linked to current profile evolution) in large tokamaks, the maximum plasma current ramp rate is 1-2 MA/s. Simultaneous ramping of the toroidal field and plasma current may relax ramp rate restrictions; limits may then be determined by power supplies.

In the following simulations the toroidal field and plasma current are ramped linearly over a 3-s startup phase that begins with toroidal field, current, and density at 10% of their final values. This is modeled by stepping the temperatures, densities, and poloidal flux forward with a fixed toroidal flux (plasma size) followed by a toroidal field compression and grid renormalization after each time step. Compressional heating and density increases are neglected since they are small. The geometric parameters are reevaluated only occasionally with an MHD equilibrium solver since they change more slowly in time. In this scenario,  $q(a_0) \approx 2.6$  is constant throughout the evolution. If  $q$  increases monotonically from the center to the edge, the toroidal field compression increases  $q(R)$  [in real space, since the compression maintains  $q(\Phi)$ ] and therefore tends to balance current diffusion, which decreases  $q$ . Sawtooth activity may then be frozen out of the startup phase, while skin current effects are eliminated.

The evolution of the central and density-averaged electron and ion temperatures is shown in Fig. 3 for Kaye-Goldston scaling in the BRAND-X device. Auxiliary power of 15 MW was applied at the end of the startup phase for a period of 3 s ( $t = 3-6$  s). After the auxiliary power is turned off, the plasma remains in a quasi-steady-state burn, which is at the bottom of the ignition window of Fig. 2. Sawtooth activity is eliminated during the startup phase and does not begin until after about 0.5 s of heating. In the burn phase, giant (~7-keV) sawteeth occur at ~1-s intervals with small (~0.5- to 1-keV) sawteeth at more frequent intervals preceding the giant sawteeth. Although this multiperiod sawtooth activity may be only an artifact of the computational model [triggering mechanism,  $q(0) < 0.95$ , and current redistribution assumptions], it is reminiscent of observations in some large experiments [15, 16]. Here, several small reconstructions occur in the plasma center before the current thrown out by the last giant sawtooth has time to penetrate and result in a large reconnection. In most cases relatively large (3- to 5-keV) sawteeth occur at about 250-ms intervals.

The evolution of the electron density is shown in Fig. 4 for this case. The density is maintained by gas fueling (equal contributions from deuterium and tritium plus small amounts of carbon and alphas) at  $(n_e) \approx 0.75n_{max}$  throughout the field startup phase, then further ramped during the auxiliary heating phase to  $n_{max}$ . The effects of the giant sawteeth can be seen in the central density, which increases between sawteeth because of a small pinch term in addition to the Ware pinch.

#### BRAND-X ( $aB_0^2/q_0 \sim 25$ ) KAYE-GOLDSTON L-MODE

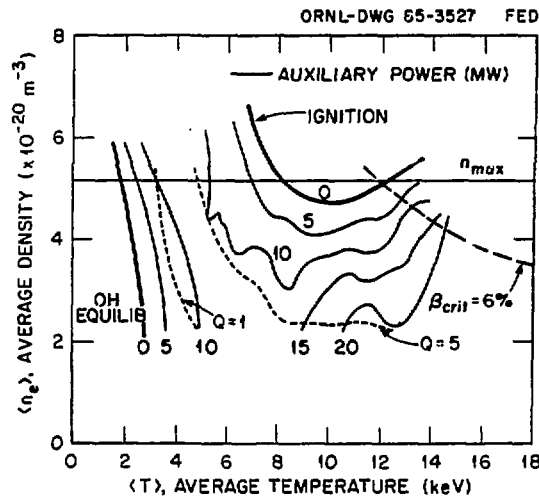


Fig. 2. Steady-state auxiliary power contours for BRAND-X with Kaye-Goldston scaling. The potential operating regime is small with the conservative limitation on density.

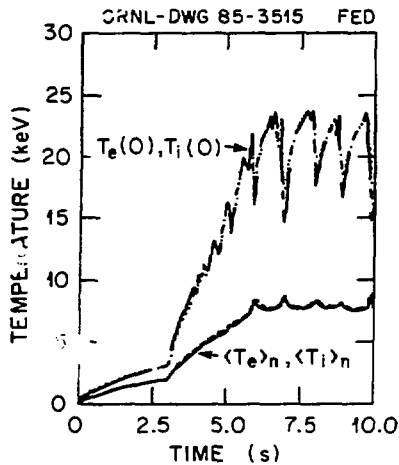


Fig. 3. Temperature evolution for the BRAND-X case with Kaye-Goldston scaling.  $P_{aux} = 15$  MW for 3 s, applied over the time interval  $t = 3-6$  s

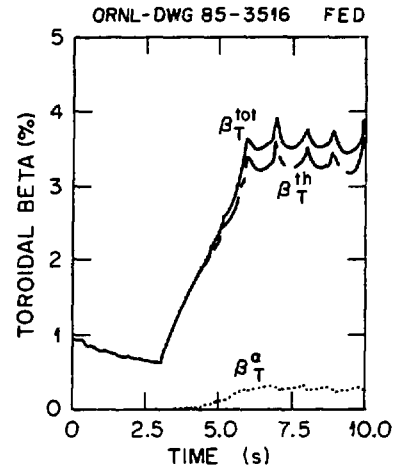


Fig. 5. Toroidal beta evolution for the BRAND-X case with Kaye-Goldston scaling. Quasi-steady burn occurs below  $\beta_{crit} \approx 6\%$ . Fluctuations include poloidal to kinetic energy conversion from giant sawteeth followed by heat pulse propagation.

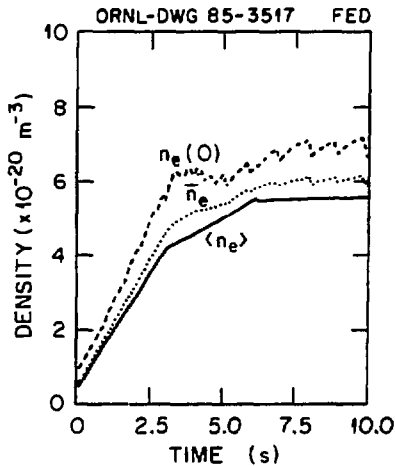


Fig. 4. Density evolution for the BRAND-X case with Kaye-Goldston scaling. The first density ramp is simultaneous with the field ramp, and the second occurs during the auxiliary heating phase.

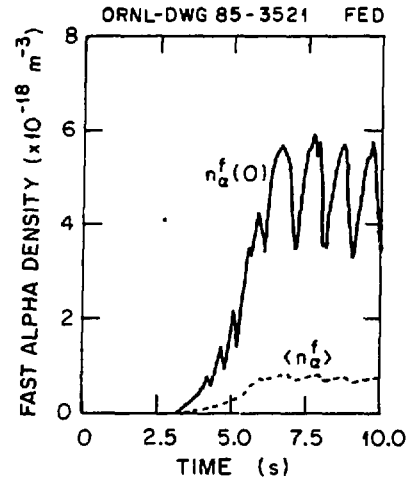


Fig. 6. Fast-alpha density evolution for the BRAND-X case with Kaye-Goldston scaling. The large fluctuations reflect the fluctuations in the fusion rate coupled with a fast-alpha slowing-down time of  $\sim 35$  ms.

Toroidal beta decreases slightly during the field ramp phase when both plasma pressure and magnetic pressure are rising, as shown in Fig. 5. The decrease in total beta after a giant sawtooth crash is governed by conduction of a heat pulse from the edge of the sawtooth region. During the burn, fast-alpha pressure represents about 10% of the total plasma pressure, although the contribution in the plasma center is somewhat greater.

The fast-alpha distribution was evolved with a time-dependent multigroup treatment of the Fokker-Planck equation assuming local, classical thermalization [17]. The central and average fast-alpha density evolutions are shown in Fig. 6. The sharp drop in fast-alpha density after each giant sawtooth in the plasma center is driven by a large reduction in the fusion rate ( $\sim 30-40\%$ ) coupled with a short thermalization time ( $\sim 35$  ms). If such pulsed activity does exist, the correlation of time-resolved fast-alpha and neutron diagnostics may provide a means of evaluating fast-alpha confinement and thermalization.

The volt-second (poloidal magnetic flux) requirements of the poloidal field system can be evaluated by integrating Faraday's law

over a surface extending from the magnetic axis to the plasma edge and then integrating over time to obtain the internal, resistive, and MHD contributions:

$$\int dt \left( \int_{\alpha} E \cdot dl = \int_0 E \cdot dl + \frac{d}{dt} \int B \cdot dA + \int B \cdot \frac{dA}{dt} \right)$$

The first term on the right becomes the time integral of the loop voltage on axis and is the resistive volt-second loss. The second term on the right yields two contributions: one is the poloidal magnetic flux in the plasma, while the other comes from step decreases in the poloidal flux due to sawtooth or other MHD activity. The final term results from changes in the geometry (tied to the toroidal flux) and is presumed to be small. The external flux must be added to these contributions to get the total flux requirement shown in Fig. 7 for the BRAND-X case being studied. Once sawtooth activity

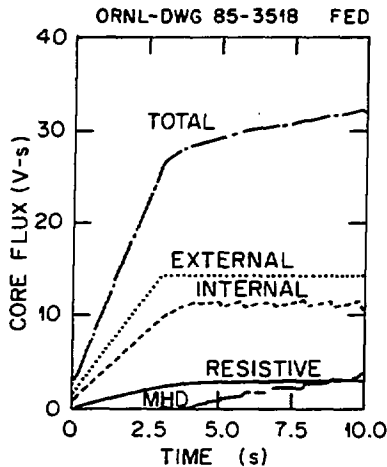


Fig. 7. Core flux (V-s) requirements for the BRAND-X case with Kaye-Goldston scaling. Sawtooth activity is the dominant dissipative mechanism during the flattop phase.

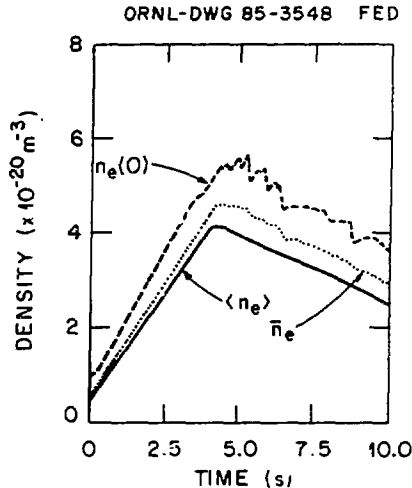


Fig. 9. Density evolution for the BRAND-X case with ohmic scaling. The density rampdown provides passive control of the thermal excursion.

starts, the internal flux is dissipated primarily by MHD activity. The total dissipative losses are about 7 V-s for this 10-s simulation, compared with about 25 V-s required to produce the internal and external fluxes. To this must be added the breakdown and resistive losses to bring the plasma to the 1-MA initial state.

Under more favorable confinement with a larger operating window, as in OH scaling, thermal runaway to pressures in excess of  $\beta_{crit}$  must be controlled in some manner. A relatively simple procedure for this is to ramp down the density as ignition is approached while the temperature increases, as illustrated in Figs. 8 and 9. Here 5 MW of auxiliary heating is applied for 3.0 s after the field ramp is complete. At  $t = 4$  s, a slow decrease in density is begun. The excursion follows just above the ignition curve of Fig. 1, and beta remains below the critical value of  $\sim 6\%$  as shown in Fig. 10.

In the lower-density, higher-temperature regime at the end of the simulation, alpha particle physics should be more easily observed. The contribution to the average pressure reaches about

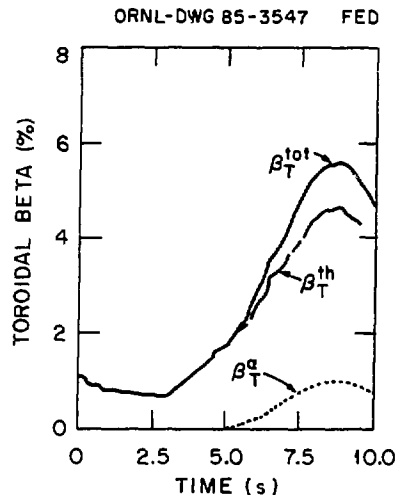


Fig. 10. Toroidal beta evolution for BRAND-X with ohmic scaling shows that density control provides a passive means of controlling  $\beta < \beta_{crit} \approx 6\%$ . The contribution by fast alphas is double that of the previous case (Fig. 5).

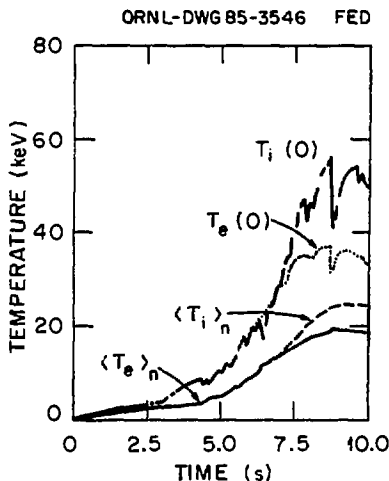


Fig. 8. Temperature evolution for the BRAND-X case with ohmic scaling. The low-density, high-temperature operation allows separation of the ion and electron temperatures.

20% with the central contribution in excess of 30%. The thermalization time in the plasma center reaches  $\sim 90$  ms, and the central fast-ion density approaches  $7.5 \times 10^{18} \text{ m}^{-3}$ , as shown in Fig. 11.

#### IV. Summary

The dynamics of ignition in magnetically confined plasmas has long been the subject of theoretical studies and much speculation. Only a few issues have been addressed here. Studies of the influence that ignition in any magnetic confinement device could provide. A compact tokamak ignition device appears to be an attractive candidate for addressing ignition in the experimental program because its susceptibility to uncertainties in confinement scaling is lower than that of tokamaks that rely heavily on auxiliary heating. A compressed startup phase consisting of simultaneous toroidal field and current ramps can be used to maximize the flattop operating time. A larger ignition window opens up a broader range of plasma dynamics and alpha particle physics.

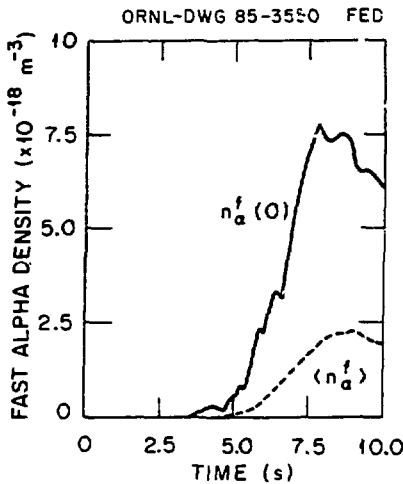


Fig. 11. Fast-alpha density evolution for the BRAND-X case with ohmic scaling shows that the longer slowing-down time ( $\sim 90$  ms), low-density, high-temperature regime leads to a much larger relative alpha population.

#### References

- [1] B. Coppi, "An Advanced Burning Core Experiment," MIT Research Laboratory of Electronics, Report PTP-84/17 (1984).
- [2] D. R. Cohn, E. Bobrov, L. Bromberg, G. Kohse, J. E. C. Williams, R. Witt, T. F. Yang, G. Listvinsky, D. Berwald, G. Bell, and C. Wagner, "Compact minimum cost ignition test reactor," *Fusion Technol.*, Vol. 8, pp. 1291-6, 1985.
- [3] Presentations at the Design Point Workshop on Compact Ignition Experiments, Boston, June 1985, unpublished.
- [4] B. Coppi, "Compact experiments for  $\alpha$ -particle heating," *Comments Plasma Phys. Controlled Fusion*, Vol. 3, pp. 47-62, 1977.
- [5] J. A. Schmidt, G. V. Sheffield, C. Bushnell, J. Citrolo, R. Fleming, C. A. Flanagan, Y-K. M. Peng, T. E. Shannon, L. Bromberg, D. R. Cohn, D. B. Montgomery, M. J. Saltmarsh, R. Mattas, L. S. Masson, J. G. Crocker, J. Anderson, and J. D. Rogers, "The toroidal fusion core experiment studies," in *Plasma Physics and Controlled Nuclear Fusion Research (Proc. 10th Int. Conf. London, 1984)*, Vol. 3 (IAEA, Vienna, 1985) 297-307.
- [6] N. A. Uckan, W. A. Houlberg, and J. Sheffield, "Physics evaluation of compact tokamak ignition experiments," this conference.
- [7] C. E. Singer, L-P. Ku, G. Bateman, F. Seidl, and M. Sugihara, "Physics of compact ignition tokamak designs," this conference.
- [8] W. A. Houlberg, S. E. Attenberger, and L. M. Hively, "Contour analysis of fusion reactor plasma performance," *Nucl. Fusion*, Vol. 22, pp. 935-45, 1982.
- [9] S. M. Kaye, "A review of energy confinement and local transport scaling results in neutral-beam heated tokamaks," *Phys. Fluids*, Vol. 28, pp. 2327-43, 1985.
- [10] C. S. Chang and F. L. Hinton, "Effect of finite aspect ratio on the neoclassical thermal conductivity in the banana regime," *Phys. Fluids*, Vol. 25, pp. 1493-4, 1982.
- [11] S. P. Hirshman, R. J. Hawryluk, and B. Birge, "Neoclassical conductivity of a tokamak plasma," *Nucl. Fusion*, Vol. 17, pp. 611-4, 1977.
- [12] M. Murakami et al., "Confinement studies of neutral beam heated discharges in TFTR," *Proc. 12th European Conf. on Controlled Fusion and Plasma Physics*, Budapest, 1985.
- [13] F. Troyon, R. Gruber, H. Saurenmann, S. Semenzato, and S. Succi, "MHD limits to tokamak confinement," *Plasma Phys. Controlled Fusion*, Vol. 26, pp. 209-15, 1984.
- [14] J. P. Christiansen, D. J. Campbell, J. G. Cordey, S. Ejima, and E. Lazzaro, "Resistivity and field diffusion in JET," *Proc. 12th European Conf. on Controlled Fusion and Plasma Physics*, Budapest, 1985.
- [15] W. Pfeiffer, "Double sawtooth oscillations in the Doublet III tokamak," *Nucl. Fusion*, Vol. 25, pp. 673-9, 1985.
- [16] D. J. Campbell et al., "Analysis of sawtooth instabilities in JET," *Proc. 12th European Conf. on Controlled Fusion and Plasma Physics*, Budapest, 1985.
- [17] S. E. Attenberger and W. A. Houlberg, "Fast alpha diffusion and thermalization in tokamak reactors," *Nucl. Technol./Fusion*, Vol. 4, Part 2, pp. 129-34, 1983.

#### DISCLAIMER

This report was prepared as an account of work sponsored by an agency of the United States Government. Neither the United States Government nor any agency thereof, nor any of their employees, makes any warranty, express or implied, or assumes any legal liability or responsibility for the accuracy, completeness, or usefulness of any information, apparatus, product, or process disclosed, or represents that its use would not infringe privately owned rights. Reference herein to any specific commercial product, process, or service by trade name, trademark, manufacturer, or otherwise does not necessarily constitute or imply its endorsement, recommendation, or favoring by the United States Government or any agency thereof. The views and opinions of authors expressed herein do not necessarily state or reflect those of the United States Government or any agency thereof.